Mass Spectrometer Composition Probe for Batch Cell Studies of Supercritical Fluid Phase Equilibria

Shean-jer Chen, Robert E. Randelman, Rober L. Seldomridge, and Maciej Radosz*

Exxon Research and Engineering Company, Annandale, New Jersey 08801

A batch cell coupled with a mass spectrometer (MS) composition probe is demonstrated for the first time for measuring high-pressure fluid-phase equilibria at temperatures up to 200 °C and pressures up to 600 bar. Compared to gas chromatography (GC), this MS composition probe requires a much smaller sample that is taken from the cell into the spectrometer. Its application is illustrated for 1-butene + ethylene. The apparatus is also tested on two additional systems, supercritical carbon dioxide + decane and supercritical propane + polyisobutene.

Introduction

The accurate measurement of phase equilibria is crucial to developing and verifying thermodynamic models, such as those utilizing equations of state. There are two different approaches to phase equilibrium measurements, continuous flow and batch. In the flow cell approach (*1*), the mixture continuously flows through a static mixer and is separated in a cell into two equilibrated phases. Both phases are continuously sampled. The flow cell approach minimizes the residence time and produces relatively large samples. However, it requires a large amount of feed, and is limited to components that easily flow. By contrast, the batch cell approach requires a small amount of feed. However, the challenge is to sample the batch cell without perturbing the state of phase equilibrium.

The overall mixture composition in the batch cell is determined either from a known initial amount of each component (synthetic method) or from sampling and analysis of the cell content (analytic method). The most common and useful analysis, especially for multicomponent mixtures (*2*), is gas chromatography (GC), either on-line or off-line. The problem associated with the on-line GC is the contamination of the cell with the carrier gas upon repeated sampling. The problem associated with the off-line GC is the need to inject the sample into a homogenizing chamber at high temperatures that may cause thermal decomposition of some components.

An on-line mass spectrometer (MS) sampling and analysis method, which is coupled directly with a high-pressure batch cell, has not been demonstrated but has been mentioned as a possibility by Deiters and Schneider (*3*). However, it has been demonstrated successfully in connection with supercritical fluid chromatography (*4*).

The goal of this work is to develop a small high-pressure batch cell applicable to polymer solutions in sub- and supercritical solvents, coupled with an MS composition probe for the light components. The driving force for the MS probe development is that, instead of injecting a sizable sample into an ambient or elevated pressure environment, as it is done in GC sampling, the MS method requires a trace amount to be pulled into a high-vacuum environment. As a result, the potential for thermal degradation prior to analysis and for perturbing the state of phase equilibrium while sampling is greatly diminished. Furthermore, MS analysis is much faster than GC analysis.

* To whom correspondence should be addressed.

Experimental Section

The main part of the apparatus is a high-pressure variable-volume optical cell where it is possible to vary the pressure and view the phase transitions at constant temperature and composition. The cell, a polished, horizontally mounted cylinder, is equipped with a movable piston to control the pressure without changing the feed composition, and with a stirring bar. The stirring bar is activated by a rotating permanent magnet which is located under the cell and driven by an air pump. After known amounts of all the components are loaded into the cell, the pressure is increased at a constant temperature, while stirring the cell content, till a homogeneous phase is formed. Upon lowering the pressure, the cloud point or bubble point phase transitions are determined visually. The temperature and feed composition corresponding to phase transition are recorded.

Cell Design. A schematic diagram of the cell is shown in Figure 1. The bore of the cell is 9.550 cm long and has a diameter of 1.905 cm. The length of the movable piston is 2.540 cm, so the total variable volume (excluding the piston volume) is 17 cm^3. The cell is made of stainless steel 304 and has four ports. Two ports are shown in Figure 1; the other two ports are in the plane that is perpendicular to that shown in Figure 1. One of the ports is used for feed; the others are used for sampling. Each port is made of an adapter (Valco Inc. Model ZTA41) that is welded to the cell. A $^1/_{16}$-in. (1.588-mm) hole is drilled through this adapter so that a piece of $^1/_{16}$-in.-o.d. (1.588-mm) tubing can be inserted to about 0.030 in. (0.762 mm) above the cell bore. The opening that connects the cell bore with this tubing has a $^1/_{32}$-in. (0.794-mm) diameter. These dimensions were chosen to minimize the volumes of the sampling lines.

The cell consists of three parts: a window cap, cell body, and end cap. A sapphire window (0.5 in., 12.700 mm, thick) is attached to the cell body with a window cap. The cell, sealed with two O-rings (Viton (i.d. × o.d. × thickness), $^{13}/_{16}$ in. × $1^1/_{16}$ in. × $^1/_8$ in., 20.638 mm × 26.988 mm × 3.175 mm), is hydrotested up to 1200 bar at ambient temperature and used up to 600 bar at 200 °C.

The clearance between the cell bore and the piston is 0.004 in. (0.102 mm). The piston is made of brass to prevent it from scratching the highly polished (by honing) surface of the bore. The piston has two O-rings ((i.d. × o.d. × thickness), $^9/_{16}$ in. × $^3/_4$ in. × $^3/_{32}$ in., 14.288 mm × 19.050 mm × 2.381 mm) to prevent the pressurizing fluid from leaking into the window side of the cell. The O-rings are made of Teflon-impregnated Viton. This internally lubricated compound

0021-9568/93/1738-0211$04.00/0

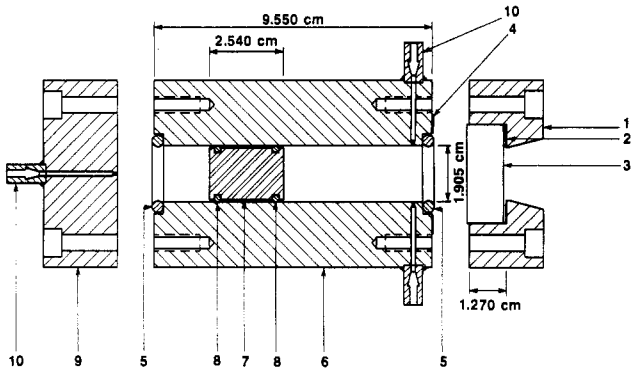

Figure 1. Schematic diagram of the batch cell: 1, window cap; 2, Garlock gasket (0.032 in. thick); 3, sapphire window; 4, copper cushion (0.010 in., 0.254 mm, thick); 5, Viton O-ring; 6, cell body; 7, piston; 8, Viton O-ring; 9, end cap; 10, Valco adapter.

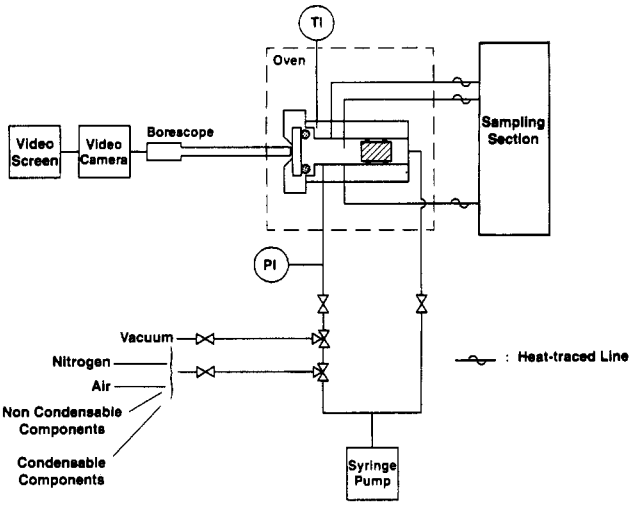

Figure 2. Simplified flow diagram of the batch cell apparatus: PI, pressure transducer and readout; TI, platinum resistance thermometer and readout. The sampling lines are heat traced.

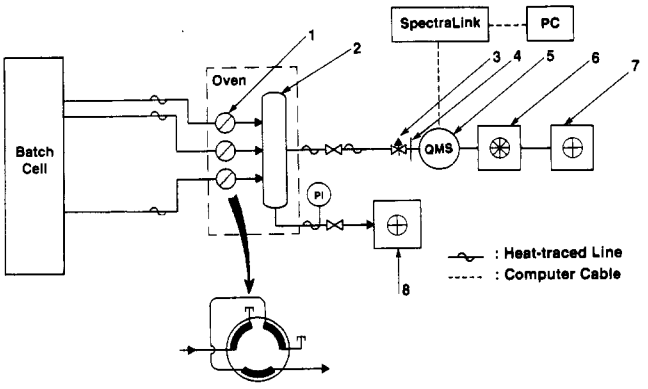

Figure 3. Sampling section with mass spectrometer: 1, Valco six-way sampling valve; 2, homogenizing chamber; 3, high-vacuum valve; 4, orifice; 5, quadrupole mass filter; 6, turbomolecular pump; 7, 8, mechanical pumps; PI, pressure transducer and readout; PC, personal computer; SpectraLink, computer interface. The lines upstream of the pumps are heat traced.

reduces rubber friction and minimizes the pressure drop across the piston.

Full Setup. A flow diagram of the batch cell apparatus is shown in Figure 2. The cell is installed in a nitrogen-purged oven (Bemco Inc.) that is equipped with a fan to ensure temperature uniformity. The oven can be controlled to within ±0.1 K. The cell temperature is measured with a platinum resistance thermometer inserted into a thermal well inside the cell body, to within ±0.1 K. The pressure is measured with a pressure transducer (Heise Model 623) to within ±0.3 bar. The pressure readings are checked against a dial gauge (Heise Model CM), which in turn is calibrated against a dead-weight tester (Ruska Corp. Model 5201-700).

The phase transitions are observed visually on a video screen, through a borescope (Instrument Technology Inc., special version based on Series 123000, modified for high-temperature applications) and video camera interface. The borescope field of view is selected in such a way that the whole chamber can be seen clearly.

The solvent is charged to the cell with a syringe pump (Ruska Corp. Model 2250). This pump allows for an accurate volume reading, and is also used as a pressure generator. In addition, there are two other syringe pumps (High Pressure Equipment Co. Models 87-6-5 and 62-6-10) available for charging condensable components. One of the condensable components is usually used as a pressurizing fluid. Non-condensable gases are charged from a PVT vessel. The amount of gas delivered to the cell is calculated from the pressure drop and the PVT properties of the gas.

Sampling Section. The sampling section, including the mass spectrometer, is shown in Figure 3. Three sampling lines (0.010-inch. 0.254-mm, i.d.) allow for taking samples from the top, bottom, and middle of the batch cell. These sampling lines are heat traced and maintained at the same temperature as the cell to avoid phase separation. The samples are rapidly depressurized and injected into a 300 cm^3 homogenizing chamber (Whitey Co. Model 304-HDF4-300) upon switching zero-volume sampling valves (Valco Inc., six-way CW series), as shown in Figure 3. Each line is purged at least three times prior to actual sampling, which was tested to be sufficient to clear the line completely. The total volume of each sampling line and the valve is estimated to be about 0.06 cm^3.

The purpose for the homogenizing chamber is to evaporate and homogenize the sample. The key requirement here is to avoid condensation by maintaining vacuum and uniformly high temperature. Therefore, the valves and the chamber are located in an oven (Hewlett-Packard Co.). A mechanical pump controls the homogenizing chamber pressure at around 0.02 kPa.

The mass spectrometer (UTI Co. Model 100C), on the other hand, pulls in the sample from the homogenizing chamber because its pressure is below 5×10^{-7} kPa. In order to minimize surface adsorption, the line between the homogenizing chamber and the mass spectrometer is heated at 150 °C. The mass spectrometer consists of a turbomolecular pump, a mechanical pump, high-vacuum valves, orifices, and a quadrupole mass filter. The mass range of this spectrometer is 1–300 amu (atomic mass unit).

The mass spectrum is transmitted to a personal computer (Hewlett-Packard, Vectra ES/12) through a computer interface (UTI Co., SpectraLink Model 100) for storage and analysis. After taking three to four samples for MS analysis, the homogenizing chamber is evacuated and purged with a new sample at least three times before the next series of MS runs.

The MS analysis is not applicable to polymeric components. In this case, a different, gravimetric–volumetric sampling method is used, which is illustrated in Figure 4. The one-phase polymer solution is injected through one of the six-way sampling valves into a glassware trap filled with glass wool. The polymer is collected in the trap while the gaseous components are collected in a graduated volumetric flask. For multicomponent systems, the collected gas is subsequently

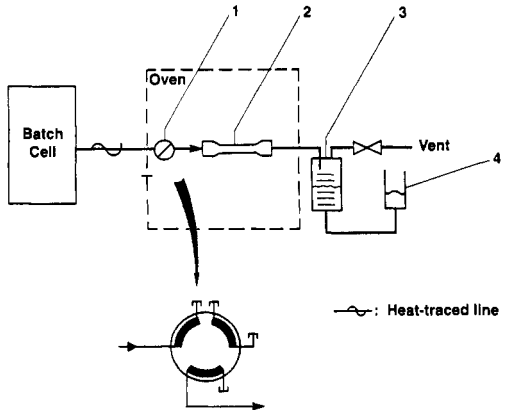

Figure 4. Gravimetric–volumetric sampling: 1, Valco six-way sampling valve; 2, glassware trap filled with glass wool; 3, graduated volumetric flask; 4, glass reservoir. The lines upstream of the Valco valves are heat traced.

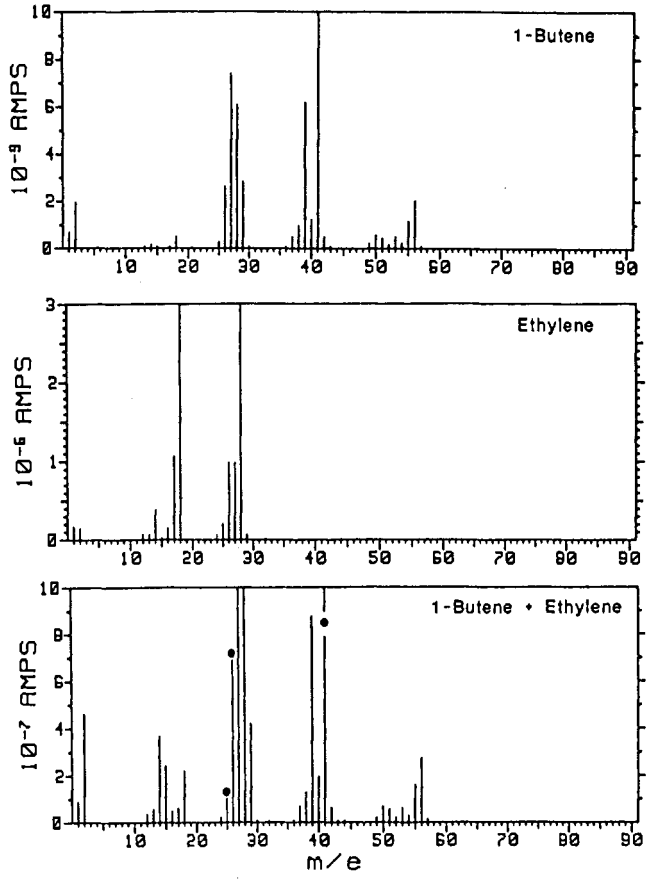

Figure 5. Mass spectra of 1-butene and ethylene at 70 eV. The peaks used for deconvolution calculations are indicated with filled circles.

analyzed by GC or MS. The overall composition of the polymer solution in mass percent is calculated from the material balance (*5*, *6*), and compared for consistency with the composition obtained from the synthetic method.

Materials. Ethylene (polymer grade, minimum purity 99.9%), 1-butene (CP grade, minimum purity 99.0%), carbon dioxide (bone dry grade, minimum purity 99.8%), and propane (CP grade, minimum purity 99.0%) were from Matheson. Decane was from Aldrich (minimum purity 99.0%). Polyisobutene was from PolySciences, Inc. According to the manufacturer, the number-average molecular weight (M_n) is 500 and the polydispersity is around 2.5. All chemicals were used as received.

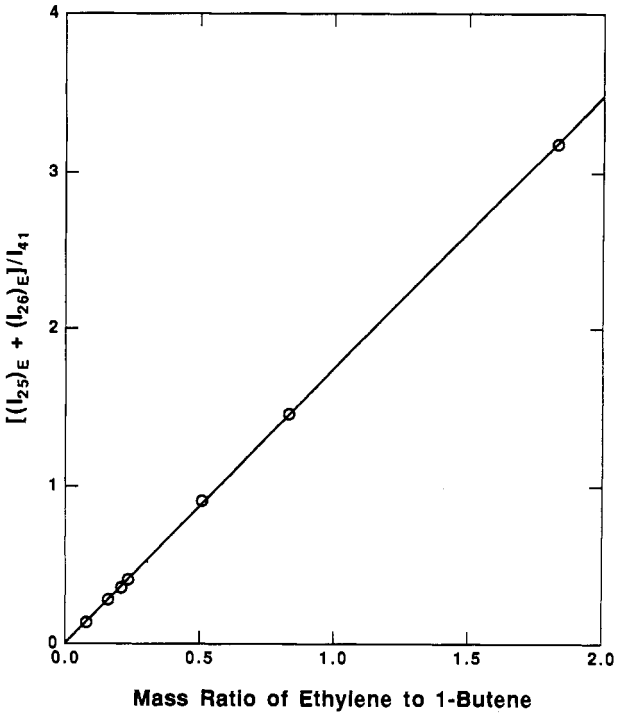

Figure 6. Results of MS analysis: the peak intensity ratio is a linear function of the mass ratio.

Results and Discussion

Two series of tests are performed to validate the apparatus, one on 1-butene + ethylene to test the MS sampling procedure, and one on supercritical carbon dioxide + decane to test the phase equilibrium procedure. Next, the apparatus is used to measure a more complex phase behavior of supercritical propane + polyisobutene, which is an example of a polydisperse system.

1-Butene + Ethylene. Examples of MS spectra in the form of the fragmentation patterns for 1-butene, ethylene, and a mixture of 1-butene + ethylene are shown in Figure 5. Each fragmentation pattern, an MS fingerprint, resulting from the breakup of a molecule by the excess energy obtained in the initial ionization collision (70 eV, in our case), can be used for qualitative and quantitative analyses.

The molecular ion of 1-butene in Figure 5 has a characteristic mass-to-charge ratio (m/e) of 56 while the molecular ion of ethylene has an m/e of 28. For 1-butene, we select the peak at $m/e = 41$, $(I_{41})°$, as our reference peak because it has the highest intensity. We express the intensities of other peaks as intensity ratios. For example, the intensity ratios of 1-butene peaks at m/e of 26 and 25, with respect to $(I_{41})°$, are calculated to be 0.193 and 0.0196, respectively. These values are in good agreement with the literature data (*7*), and are used in our mixture deconvolution calculations.

For ethylene, on the other hand, we do not select the peak at $m/e = 28$ as our reference peak, even though it has the highest intensity. This is because the intensity ratios of other peaks with respect to this peak are somewhat lower than the literature data. This indicates that the measured intensity of the reference peak, $(I_{28})°$, is too high, which may be due to a trace amount of nitrogen in the system, even though the nitrogen spectrum has been subtracted as a background. Instead, we select the sum of peak intensities at m/e of 25 and 26, $(I_{25} + I_{26})°$, as our reference intensity for ethylene.

The MS spectrum of the mixture is a hybrid of the individual spectra of 1-butene and ethylene. There are several ways to deconvolute such a mixture spectrum. For example, we choose the peak at $m/e = 41$ as the characteristic peak of 1-butene because it has the highest intensity and no overlap

Table I. Bubble Pressures for Carbon Dioxide (1) + Decane (2) Measured in This Work[a]

T/°C	P/bar	T/°C	P/bar
71.1	97.4	137.8	151.2
104.4	129.4	171.1	163.8

[a] The carbon dioxide mole fraction is 0.675.

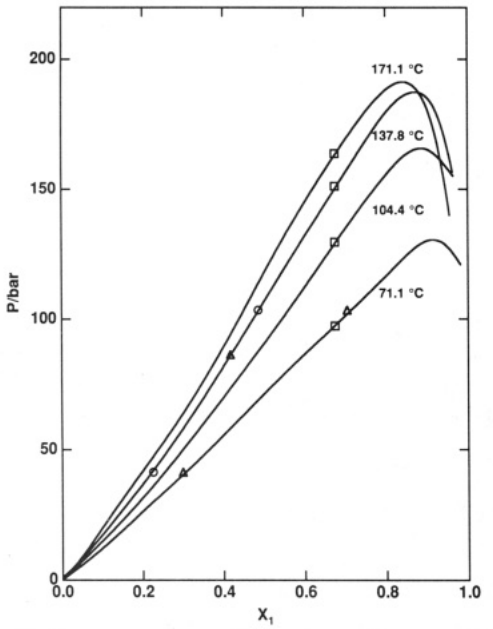

Figure 7. Pressure–composition phase diagram of CO_2 + decane: triangles, flow cell, Yu et al. (1989); circles, flow cell, Radosz (1985); squares, batch cell, this work. X_1 is the CO_2 mole fraction in the liquid phase. The solid curve represents the data measured in a batch cell by Reamer and Sage (1963).

with other species, such as ethylene and air. On the other hand, the characteristic peaks for ethylene are chosen at m/e of 26 and 25 because of low overlap with 1-butene and no overlap with air. The intensity fractions due to 1-butene for these two peaks, $(I_{25})_B$ and $(I_{26})_B$, can be estimated as follows:

$$(I_{25})_B = I_{41}[(I_{25})_B°/(I_{41})_B°] \quad (1)$$

$$(I_{26})_B = I_{41}[(I_{26})_B°/(I_{41})_B°] \quad (2)$$

where the degree sign indicates a pure component, and the subscript B represents 1-butene.

The intensity fractions due to ethylene, on the other hand, for those two peaks, $(I_{25})_E$ and $(I_{26})_E$, can be estimated as a difference between the total mixture intensities and the 1-butene intensity fractions, as follows:

$$(I_{25})_E = I_{25} - (I_{25})_B \quad (3)$$

$$(I_{26})_E = I_{26} - (I_{26})_B \quad (4)$$

Our hypothesis is that the intensity of the mixture peak at m/e = 41, I_{41}, is proportional to the partial pressure of 1-butene, and that the sum of the ethylene intensities, $[(I_{25})_E + (I_{26})_E]$, obtained from eqs 1–4, is proportional to the partial pressure of ethylene. Therefore, $[(I_{25})_E + (I_{26})_E]/I_{41}$ is expected to be proportional to the partial pressure ratio of ethylene to 1-butene and, hence, to the mass ratio of ethylene to 1-butene.

In order to test this hypothesis, we plot $[(I_{25})_E + (I_{26})_E]/I_{41}$ versus the mass ratio of ethylene to 1-butene for seven mixtures of known composition in Figure 6. The solid line obtained from least-squares regression goes through the origin, as it should. The slope of this line depends on the MS instrument specifications, such as ionization efficiencies,

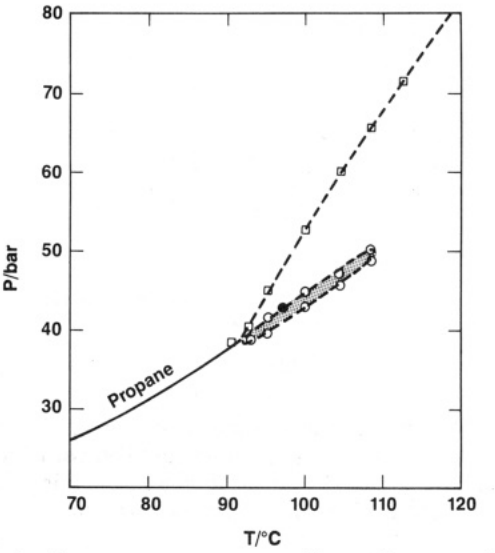

Figure 8. Pressure–temperature phase diagram of polyisobutene (27.1 wt %) in propane: squares, two-phase boundary; circles, three-phase boundary. The heavy curve is the propane vapor pressure curve, and the bold dot is the propane critical point. The shaded band near the propane critical point is the three-phase VLL region.

Table II. Phase Boundary Pressures for the Propane + Polyisobutene System Shown in Figure 8[a]

	P/bar		
T/°C	two-phase boundary	three-phase boundary	three-phase boundary
90.5	38.5		
92.8	40.5	39.7	39.0
95.4	45.0	41.6	39.5
100.0	52.7	44.8	43.2
104.5	60.3	47.0	45.5
108.5	65.7	50.0	48.7
112.5	71.5		

[a] The polyisobutene mass percent is 27.1.

multiplier gains, and quadrupole transmission. On the basis of the data supplied by the UTI manufacturer, the slope is estimated to be between 1.806 and 1.408. The value obtained from our calibration, 1.743, falls in this range.

This example demonstrates that mass spectrometry can be used as a quantitative composition probe. To sum up, the calibration procedure is as follows: (a) run the mass spectra of pure components, (b) choose the peaks that represent each component uniquely and determine their intensity ratios, (c) make up mixtures of known composition and correlate the peak intensity ratios and the mass ratios, and (d) run the spectrum of an unknown mixture and estimate its composition from the intensity ratio versus mass ratio correlation. While this procedure is derived for binary mixtures, it is also applicable to multicomponent mixtures (*8*).

Carbon Dioxide + Decane. This batch cell is also tested on carbon dioxide (1) + decane (2). Phase equilibrium data for this system are reported by Reamer and Sage (*9*), and subsequently confirmed by Sebastian et al. (*10*), Radosz (*1*), and Yu et al. (*11*). The bubble pressures for x_1 = 0.675 measured at four temperatures, 71.1, 104.4, 137.8, and 171.1 °C, are listed in Table I, and are compared with literature values in Figure 7. As shown in this figure, the measured pressures are in excellent agreement with literature values; the largest discrepancy is within the pressure transducer accuracy. In this case, x_1 is determined from gravimetric–volumetric sampling (analytic technique) after the measurements. Since gravimetric–volumetric sampling is found to

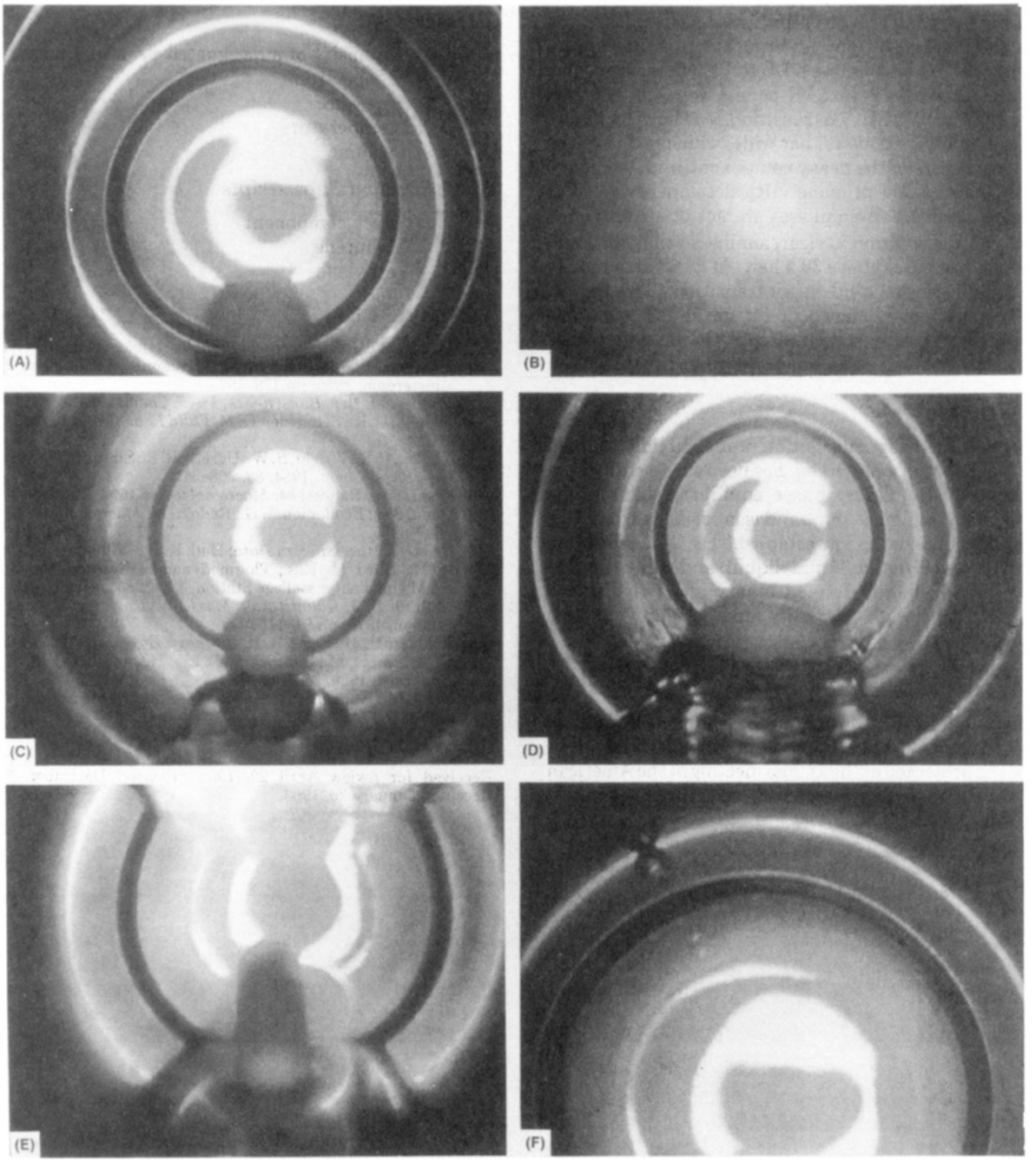

Figure 9. Phase transitions of polyisobutene + propane on going from a high to a low pressure: (A) clear one-phase solution; (B) cloud point; (C) two-phase region, polymer-rich bottom phase and propane-rich top phase; (D) upon lowering pressure, interface is going up, more heavy phase accumulates; (E) three-phase region, vapor phase at the top; (F) VL phase transition. The bright rings are due to reflection from the sapphire window and the polished surface of the piston. The magnetic stirring bar and O-ring can be seen in all the pictures except in (B).

be a straightforward and reliable approach, no attempt is made to use MS sampling for carbon dioxide + decane.

Propane + Polyisobutene. Since our goal is to use this apparatus with polymeric systems, the final test is an example of phase equilibrium measurements for a mixture of supercritical propane + polyisobutene (PIB). This system exhibits liquid–liquid (LL) immiscibility around the propane critical temperature, due to the dissimilarity of free volume, as described by Chen and Radosz (*5*).

A pressure–temperature phase diagram measured in this work for 27.1 mass % PIB in propane is shown in Figure 8, including vapor–liquid (VL), liquid–liquid (LL), and vapor–liquid–liquid (VLL) phase boundaries. The solid curve is the propane vapor pressure curve, and the filled circle is the propane critical point. The data shown in Figure 8 are listed in Table II.

Consider the three-phase transitions at a constant temperature of 95.4 °C. For example, the solution is clear at higher pressures, as shown in Figure 9A, but it turns cloudy, as shown in Figure 9B, when the pressure is reduced to 45.0 bar, indicating the onset of phase separation. A bulk phase disengagement is observed when the pressure is further reduced below the cloud point pressure. The mixture separates into a polymer-rich bottom phase and a solvent-rich top phase, as shown in Figure 9C. The disengagement time below the cloud point is between 30 and 45 min. Pressure reduction causes the interface to rise, as shown in Figure 9C,D, which indicates a dew-point-like transition, where one

observes the onset and growth of the high-density phase upon lowering the pressure. Upon lowering the pressure to 41.6 bar, still at 95.4 °C, we observe a LL to VLL transition. The VLL phases shown in Figure 9E persist down to 39.5 bar, where we observe a VLL to VL transition. As shown in Figure 8, the VLL region is about 1.6 bar wide, which is due to the polydisperse nature of the heavy component, and extends to about 12 K above the propane critical temperature. For example, at 112.5 °C, three phases are not observed.

At 90.5 °C, the solution is clear, similar to that shown in Figure 9A, at pressures above 38.5 bar. At 38.5 bar, a bubble is formed, indicating a liquid–vapor transition. This bubble pressure experiment is shown in Figure 9F. The bubble pressure point virtually coincides with the propane vapor pressure, and is shown as an open square in Figure 8.

Conclusions

A mass spectrometer composition probe, directly coupled with a variable-volume batch cell, has been successfully used to determine high-pressure phase equilibria. This probe requires a much smaller sample, and is much faster than GC, but its calibration is not as well established as GC calibration. Examples of vapor–liquid, liquid–liquid, and vapor–liquid–liquid equilibria, in well-defined binary and polydisperse systems, illustrate the versatility and accuracy of this apparatus.

Acknowledgment

We are grateful to C. K. Morgan, E. C. Ponce, and Dr. S. H. Huang for helpful discussions. A preliminary account of this work was presented at the annual meeting of the American Institute of Chemical Engineers, Chicago, 1990.

Glossary

I	intensity of a designated peak in a mass spectrum
P	pressure
T	temperature
V	volume

Subscripts and Superscripts

°	pure component
B	1-butene
E	ethylene

Literature Cited

(1) Radosz, M. In *Supercritical Fluid Technology*; Penninger, J. M. L., Radosz, M., McHugh, M. A., Krukonis, V. J., Eds.; Elsevier: Amsterdam, 1985; pp 179–190.
(2) Radosz, M. *Ber. Bunsen-Ges. Phys. Chem.* **1984**, *88*, 859–862.
(3) Deiters, U. K.; Schneider, G. M. *Fluid Phase Equilib.* **1986**, *29*, 145–160.
(4) Yonker, C. R.; Wright, B. W.; Udseth, H. R.; Smith, R. D. *Ber. Bunsen-Ges. Phys. Chem.* **1984**, *88*, 908–911.
(5) Chen, S.-j.; Radosz, M. *Macromolecules* **1992**, *25*, 3089–3096.
(6) Chen, S.-j.; Economou, I. G.; Radosz, M. *Macromolecules* **1992**, *25*, 4987–4995.
(7) *Selected Mass Spectra Data*; Hall, K. R., Wilhoit, R. C., Ferguson, A. M., Boyd, B., Eds.; Thermodynamics Research Center, Texas A&M University: College Station, TX, 1983; Serial Nos. 23 and 25.
(8) Millard, B. J. *Quantitative Mass Spectrometry*; Heyden & Son: London, 1978; pp 91–115.
(9) Reamer, H. H.; Sage, B. H. *J. Chem. Eng. Data* **1963**, *8*, 508–513.
(10) Sebastian, H. M.; Simnick, J. J.; Lin, H.-M.; Chao, K.-C. *J. Chem. Eng. Data* **1980**, *25*, 138–140.
(11) Yu, J. M.; Huang, S. H.; Radosz, M. *Fluid Phase Equilib.* **1989**, *53*, 429–438.

Received for review April 20, 1992. Revised December 28, 1992. Accepted January 26, 1993.